Difference in developmental dynamics between subcutaneous and abdominal adipose tissues in goose (*Anser Cygnoides*)

Weiran Huo,[*] Kaiqi Weng,[*] Tiantian Gu,[*] Yu Zhang,[*] Yang Zhang,[*] Guohong Chen,[*,†] and Qi Xu[*,1]

[*]*Key Laboratory of Animal Genetics and Breeding and Molecular Design of Jiangsu Province, College of Animal Science and Technology, Yangzhou University, Yangzhou 225009, China; and [†] Joint International Research Laboratory of Agriculture and Agri-Product Safety, the Ministry of Education of China, Yangzhou University, Yangzhou, Jiangsu 225009, China*

ABSTRACT Goose (*Anas cygnoides*), as a typical species domesticated from a migratory bird, has maintained the capability of depositing excess lipid and preferentially accumulating fat within the abdomen and subcutaneous, which not only leads to decrease in yield of meat product, but also affects the feed conversion rate. Here, an experiment was conducted to examine the difference in developmental dynamics between subcutaneous (**SAT**) and abdominal adipose tissues (**AAT**) in goose. The results showed that SAT could be clearly observed at embryonic days (E) 15, whereas AAT were clearer until E20. Although the weights of SAT and AAT showed a significant rising with advancing age ($P < 0.05$), their gains were not completely uniform, and more adipose deposited preferentially toward AAT after birth ($P < 0.05$). Additionally, a clear expansion in adipocyte size was observed in AAT and SAT during embryonic stages ($P < 0.05$). The average adipocyte area in AAT continued to increase after birth ($P < 0.05$), while the cell areas in SAT were relatively invariable ($P > 0.05$). Furthermore, the expression levels of *FABP4/aP2*, *ACSL1* and *PPARγ* were much higher in SAT than in AAT, whereas relative higher expression level of *IL-6* was observed in the AAT during embryonic stages. After birth, the more expression of *LPL* and *PPARα* were detected in AAT than did in SAT ($P < 0.05$), whereas greater *ATGL* expression was in SAT ($P < 0.05$). Taken together, these findings suggest that AAT may display greater fat storage capacity than SAT accompanied by changes in cell area and lipogenic capacity. Considering that there is disparity in the individual adipose tissues, we suggested that careful consideration for the precise interventions used to control SAT or AAT deposition in meat-producing animals to improve feed efficiency.

Key words: goose, adipose tissues, development, cellularity, metabolism

INTRODUCTION

During the past 20 yr, adipose tissue has become the subject of intensive research, which has been recognized as an important endocrine organ involved mainly in the control of weight regulation in mammals and poultry (Cannon and Nedergaard, 2004; Wronska and Kmiec, 2012). Understanding development of adipose tissue is crucial for curing obesity in humans and controlling fat deposition in meat-producing animals to yield higher quality meat with improved feed efficiency (Zhang et al., 2015). Unlike other organs, adipose tissue is compartmentalized into discrete depots distributed throughout the body as subcutaneous, abdominal, intermuscular (between the muscles), or intramuscular (within the muscle) fat in chickens and some other avian species. However, evidence has now accumulated to indicate that adipose tissue located in different anatomical locations of the body appear to have distinct physiological, cellularity and metabolic properties (Majka et al., 2011; Billon and Dani, 2012). For example, there are site-specific differences in adipose development, with larger adipocytes in subcutaneous adipose tissue (**SAT**) at 4 d post-hatch, more rapid growth of abdominal adipose tissue (**AAT**) in broiler chickens (Bai et al., 2015). In this context, making detailed study on physiological, cellularity and metabolic properties of these separate depots could offer potential interventions to the partition of fat between depots and its distribution.

According to published data, geese meat consumption has been increased in Asia and Europe (FAO-STAT, 2020). To judge from recent estimates, the leading geese meat consumed in the world is China, with vast majority

(95.2%) of the approximately 2.52 million tons of geese meat consumed annually (Orkusz et al., 2017). Compared with other terrestrial poultry (for example, chicken), geese possess uniquely adipose deposit traits. As a typical species domesticated from a migratory bird, goose (*Anas cygnoides*) has maintained a strong adipose deposit from their ancestors and preferentially accumulating fat within the abdomen and subcutaneous (Webster et al., 1992; Lu et al., 2015; Yu et al., 2020). However, the developmental changes that occur in individual adipose tissue during geese growth have not been evaluated. To reduce adipose deposit and improve feed efficiency, we conducted a research study to better understand the difference in developmental dynamics between SAT and AAT in goose. Therefore, our research would provide new insight for the precise interventions used to control SAT or AAT deposition in meat-producing animals to improve feed efficiency.

MATERIALS AND METHODS

Ethical Statement

All experimental procedures performed in this study were approved by the Institutional Animal Care and Use Committee of Yangzhou University (approval number: 151-2014, Government of Jiangsu Province, China). All experimental geese were managed and handled according to the guidelines established and approved by the Administration of Affairs Concerning Experimental Animals (Yangzhou University, China, 2012).

Birds and Sampling

Yangzhou geese were raised in the conventional method of stocking at the Yangzhou Tiange Goose Industry Development Co., Ltd., Gaoyou, China. 1-day-old Yangzhou goslings were grown under controlled conditions, with free access to water and feed, until 4 wk. Temperature was maintained at placement at 32°C using a controlled heater and was gradually reduced to ensure comfort. After that, the geese were maintained under natural daylight and temperatures. The feed and water were given during the daytime, when the geese were released to an open outdoor area. All geese were fed the same commercial diet (Table 1), which was formulated according to the specifications of Wang et al. (2010) and Liu et al. (2011). Embryonic days (E) 10, 15, 20 and 30 and post-hatch days (P) 1, 28, 70, 120 were investigated in this study. At each time point, 6 female geese were randomly selected for sampling. A primer set that targets a conserved region of chromobox-helicase DNA-binding gene (CHD1) gene which links to sex of poultry was designed for sex identification (Liu et al., 2014). The primer pair F (5′- TGCAGAAGCAA-TATTACAAGT-3′) and R (5′- AATTCATTAT-CATCTGGTGG-3′) respectively. PCR amplification produced a single band for males and two bands for females. The geese were transported from the farm to the experimental slaughterhouse by vehicle. Six hours before slaughter, geese were allowed access to only water. SAT

Table 1. Ingredient and nutrient composition of the experimental diets.

Item	1 to 28 d old	29 to 120 d old
Ingredients (%)		
Corn	64.0	61.5
Soybean meal	27.0	13.6
Fish meal	3.0	3.0
Alfalfa meal	2.0	16.0
Soybean oil	0.0	2.0
Dicalcium phosphate	1.8	1.9
Limestone	0.9	0.8
Salt	0.3	0.2
Vitamin and trace mineral mix	1.0	1.0
Nutrient levels		
Apparent ME, KJ/ kg	11.18	11.25
CP, %	19.0	15.1
Crude fiber, %	3.1	5.2
Ca, %	1.03	1.05
Total P, %	0.50	0.49
Salt, %	0.37	0.31
Lys, %	1.02	0.74
Met, %	0.45	0.43

Vitamin and trace mineral mix supplied the following per kilogram of total diet: vitamin A, 20,000 IU; vitamin D_3, 4,500 IU; vitamin E, 300 IU; vitamin K_3, 20 mg; vitamin B_1, 10 mg; vitamin B_2, 120 mg; vitamin B_6, 20 mg; vitamin B_{12}, 0.2 mg; nicotinic acid, 600 mg; pantothenic acid, 180 mg; folic acid, 10 mg; folate, 10 mg; biotin, 0.8 mg; choline, 7 g; Fe, 1.2 g; Cu, 0.2 g; Mn, 1.9 g; Zn, 1.8 g; I, 10 mg, Se, 6 mg.

(after peeling back the skin above the cloaca and removing all exposed adipose from both leg at the shank joints) and AAT (after peeling back the skin above the cloaca and removing all exposed adipose tissue includes the abdominal fat pad and adipose tissue collected from the walls of the gizzard) were weighed and weights were converted into a percentage of the body weight. Once weighed, all the adipose tissues were divided into three samples. One sample was placed in liquid nitrogen and then stored at −80°C for total RNA isolation. The second sample was cut into fragments weighing 1 g each and stored at −80°C for lateral analysis of triglyceride (**TG**) content. The last sample was used for the preparation of the sections and hematoxylin and eosin (H&E) analysis.

Adipose Tissue Histology Analysis

E10 was chosen as the starting point for an examination of adipose development when the embryos could be clearly identified. Stereomicroscopic examinations were carried out at E10, E15, E20, E30 and P1 (1 d post-hatch). The AAT and SAT for imaging and adipose tissue specimens from E20, E30, P1, P28, P70, and P120 geese were fixed in 4% paraformaldehyde for 24 h at room temperature, embedded in paraffin, cut at thicknesses of 5 microns, and stained with H&E. Representative areas were photographed under a Nikon 90i microscope (Nikon, Tokyo, Japan) at a magnification of 200 × . The average surface area of 250 adipocytes in each section was analyzed with Image-Pro Plus 6.0 software (Media Cybernetics, Bethesda, MD). Adipocyte density and the size distribution pattern for each image were also recorded.

Table 2. The primers used in this study.

Genes	GenBank accession	Primer sequence (5′→3′)	Length (bp)	Product size (bp)
PPARγ	AF481798	F: AGGAGCAGAACAAAGAGGTAGCA	23	158
		R: ATGGACACCGTATTTCAGGAGAG	23	
PPARα	AF481797	F: TCCCTTTTTGTCGCTGCCAT	20	100
		R: TCAGTACGTGCACAATGCTCT	21	
FAS	EU770327	F: TATCAAATGGGACCACAG	18	203
		R: CCAGAGATTGCCAAGCC	17	
ACSL1	GQ891991	F: GGAGGAAGAGTAAGGCTGATGGT	23	146
		R: CCAGGAACCGACAGTGAGCAT	21	
aP2/FABP4	AF432506	F: ATGAAAGAGCTGGGTGTGGG	20	179
		R: TGTCATCTGCTGTGGTCTCA	20	
LPL	JF343526	F: TTCGAGCTCAGCAGCACTAC	20	91
		R: CCAGACTGTACCCCAGCAAG	20	
IL-6	JF43764	F: AACTCTCCAGTGGGCTTTTC	20	135
		R: TCACCATCTGCCTTATCGTC	20	
ATGL	HQ914789	F: CACCTCTACCGCCTCTCGAA	20	198
		R: TCTCCGCACAAGCCTCCATA	20	
β-actin	M26111	F: GAGAAATTGTGCGTGACATCA	21	152
		R: CCTGAACCTCTCATTGCCA	19	

Note: All the primers are designed with Primer 5.0 software and synthesized by Shanghai Sangon bioengineering company. F: forward primer; R: reverse primer.

TG Content Analysis

The total TG content was analyzed using a triglyceride content determination kit (Beijing Solarbio Life Sciences Co., Ltd., Beijing, China) following the manufacturer's protocols. Briefly, approximately 0.1 g tissue samples were washed using PBS and reacted with the 1 mL reagents provided. After centrifugation (10 min at 8000 rpm, 4°C), the supernatant was collected for an enzymatic assay. Absorbance was measured at 420 nm using a microplate reader (Tecan, Switzerland) to establish the TG content. The TG content per g (mg/ g) was calculated as follows: TG (mg/ g) = (A $_{measure\ sample}$−A $_{blank\ sample}$) / (A $_{standard\ sample}$−A $_{blank\ sample}$) / W $_{sample\ weight}$. Three biological replicates were tested and each sample was assayed in triplicate to ensure reproducibility.

Gene Expression Analysis

Total RNA was extracted from each muscle sample using Trizol reagent (Invitrogen, San Diego, CA) according to the manufacturer's instructions. First-stand cDNA was synthesized using a cDNA synthesis kit (Takara Biotechnology Co. Ltd., Dalian, China) following the manufacturer's instructions. The newly synthesized cDNA product was immediately stored at −20°C for quantitative real-time PCR (qRT-PCR). qRT-PCR was used to detect the gene expression levels using the SYBR Green Master Mix (Vazyme, Nanjing, China) in the Quant Studio 5 (Applied Biosystems, Thermo Fisher Scientific). The mRNA abundance of lipid metabolism genes including lipoprotein lipase (**LPL**), adipocyte P2 (*aP2*, also known as fatty acid-binding protein 4, **FABP4**), long-chain acyl-CoA synthetase 1 (**ACSL1**), peroxisome proliferator-activated receptor-α/γ (*PPARα/γ*), fatty acid synthase (**FAS**), adipose triglyceride lipase (**ATGL**) and interleukin-6 (**IL-6**) were detected. All the primer sequences mentioned above were designed Primer Express 5.0 software (Applied Biosystems) based on the National Center for Biotechnology Information published sequences (www. ncbi.nlm.nih.gov, Table 2). The thermal program for qRT-PCR was 95°C for 5 min, 30 cycles of 95°C for 10 s, and 60°C for 30 s, and a final cycle of 95°C for 15 s, 60°C for 60 s and 95°C for 15 s. The *β-actin* gene was used as the reference gene to normalize the expression data, which was calculated with the $2^{-\Delta\Delta CT}$ method was employed (Livak and Schmittgen, 2001). All reactions were completed in triplicate, and the data represent the mean of three independent experiments.
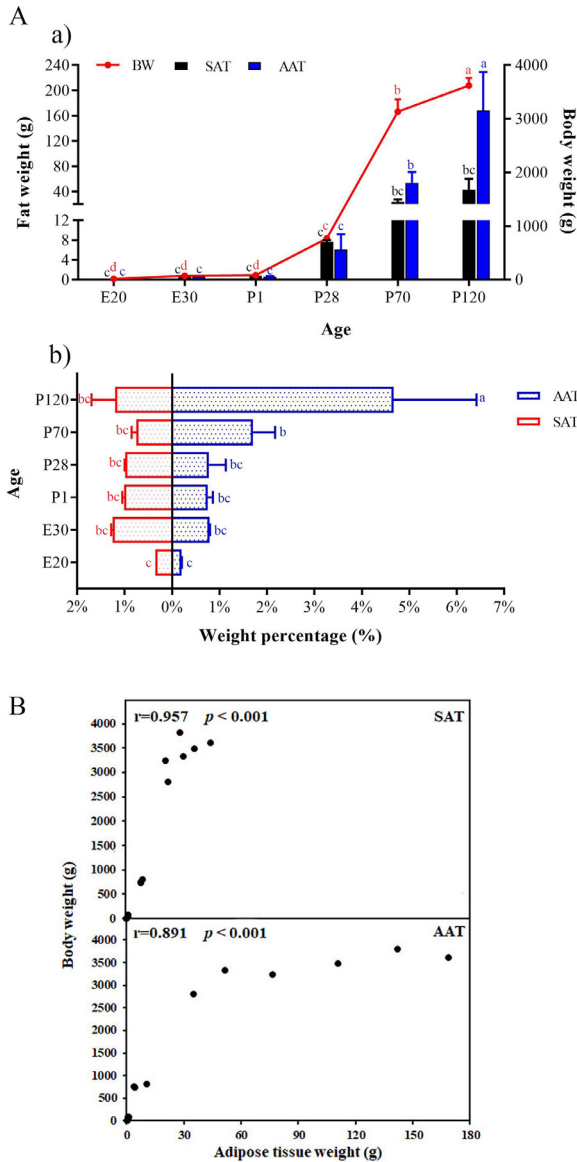
Statistical Analysis

The results are presented as mean ± standard error (SE) of the mean. The data were subjected to one-way or two-way analysis of variance (ANOVA) using SPSS 22.0 software (SPSS, Chicago, IL) and significant means were compared Duncan's multiple range test of the same software. P values < 0.05 were considered to be statistically significant.

RESULTS

Change in Adipose Tissue Weights During Growth

To evaluate the morphological changes in AAT and SAT, their development and total triglyceride content were analyzed during embryonic and post-hatch stages of geese. The results showed SAT could be clearly observed at embryonic days 15 (E15) according to their anatomic features, whereas AAT were clearer until E20 with embryonic development proceeded (Supplementary Figure 1). As development proceeded, the amount of AAT and SAT increased.

There was an interaction of age and adipose tissue depots ($P < 0.001$) on absolute adipose tissue weights and weights as a percentage of body weight (Figure 1A). The adipose depots showed a significant rising in weight
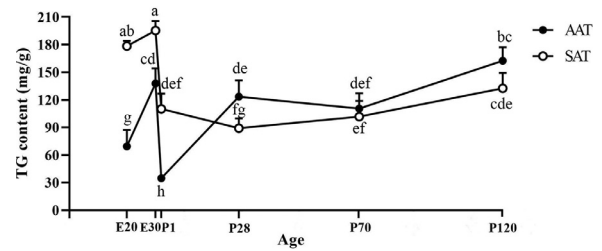
Figure 2. Triglyceride content of abdominal (AAT) and subcutaneous (SAT) adipose tissue. Data are mean ± SE (n = 3). A level of $P <$ 0.05 was set as the criterion for statistical significance.

and age) for the TG content of depots (Figure 2). There were obvious differential dynamic patterns in TG content: the total content in the AAT and SAT peaked in prenatal geese (E30) and dropped sharply in newborn geese (P1) after birth. However, the TG content in the AAT was significantly higher than that in the SAT from day 28 backward ($P < 0.05$).

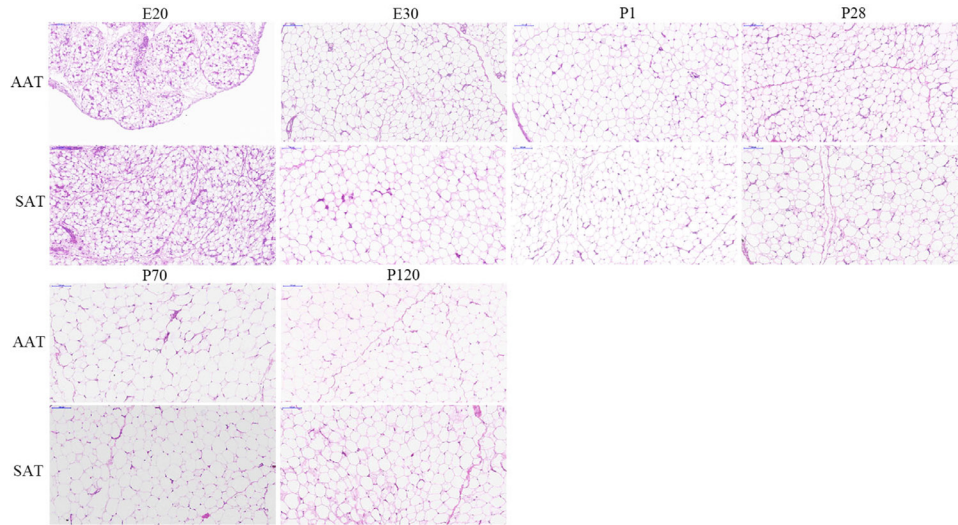## The Histology of Adipocyte Morphology During Growth

To understand adipocyte cellularity characteristics of adipose tissue depots, the amount and the distribution of adipocyte were investigated. As shown in Figure 3, the gross histology of adipocyte morphology revealed that both SAT and AAT adipocytes were presented as single adipocytes, and there were many highly-vascularized clusters of what appear to be preadipocytes in AAT and SAT of E20. A clear expansion in adipocyte size was observed in AAT and SAT, with the unilocular adipocytes of SAT were densely packed in a polyhedron shape, whereas those of AAT were spherical in shape and there still seemed to be space left for additional lipid fillings at P120.

Adipocyte Cellularity Characteristics of Adipose Tissue Depots During Growth

The data from the cell size measurements of AAT and SAT supported the microscopic observations (Figure 4). The average cell size in AAT and SAT sections increased significantly during embryonic stages ($P < 0.001$). Adipocyte size and number are negatively correlated with each other, and the average number of adipocytes decreases markedly during this same time frame (AAT, $P < 0.001$ and SAT, $P = 0.001$, respectively). After birth, the average cell area in AAT continued to increase. However, a kind of stationary period between P70 and P120 was observed in SAT, which did not show any enlargement in average cell area ($P = 0.268$). The average number of adipocytes had almost no changes in AAT and SAT after birth ($P = 0.175$).

To determine the contribution of adipocyte size to adipose tissue mass, we next quantified the diameter distributions (Figure 5). All diameter distributions for AAT and SAT adipocytes were biphasic, and a large proportion of small cells appeared during embryonic

Figure 1. Allometric development of subcutaneous (SAT) and abdominal adipose tissue (AAT). (A) Body weight, abdominal and subcutaneous adipose tissue absolute weights (a) and weights as a percentage of body weight (b) during embryonic and post-hatch development. (B) Correlations between adipose tissue weight and body weight in geese. Data are mean ± SE (n = 3). Bars with different letters are significantly different ($P < 0.05$).

with advancing age, and they gained to relatively different degrees, especially at the age of 28 days thereafter in AAT. In addition, the relationship between adipose tissue depot weights and BW was also determined (Figure 1B). The significant correlation was observed between the weight of the AAT and body weight, as well as between AAT and body weight (r = 0.957, $P < 0.001$ and r = 0.891, $P < 0.001$, respectively).

Comparison of the Lipid Content During Growth

We also quantified the total TG accumulation of SAT and AAT from E20 to P120. There was a significant interaction ($P < 0.001$) between factors (adipose depots
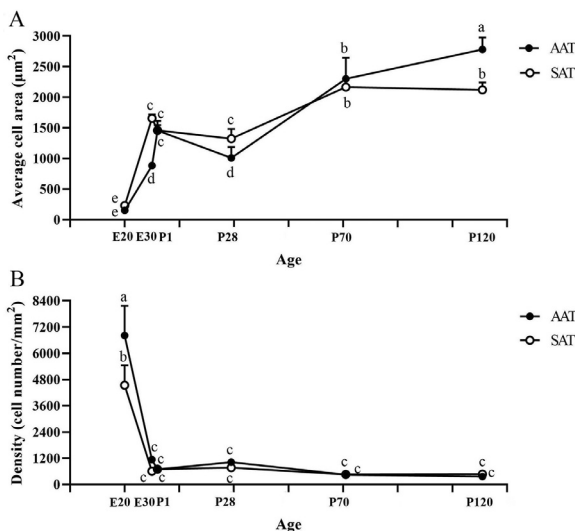
Figure 3. Hematoxylin-eosin-stained sections of abdominal (AAT) and subcutaneous adipose tissue (SAT) during embryonic and post-hatch development. Magnification of $200 \times$ was used (Bar = 100 mm).

stages. During the embryo development, the cell diameter distributions showed a sharp cutoff below 20 μm in diameter. The proportion of large adipocytes than 70 μm increased rapidly after birth. Analysis of distribution was different in AAT and SAT. At P120, approximately 70% of the adipose tissue mass in SAT was attributable to the volume of adipocytes >40 μm in diameter, whereas adipocytes >40 μm in diameter comprised most of the tissue mass in AAT (90%).

Expression Levels of Genes Associated With Lipid Deposition and Removal of Adipose Tissue During Growth

To further dissect out the mechanisms underlying involved in lipid deposition and removal, the mRNA

Figure 4. Adipocyte cellularity in abdominal (AAT) and subcutaneous adipose tissue (SAT) during embryonic and postnatal development. (A) Mean adipocyte size (area, μm^2) and (B) adipocyte number (density, per mm^2). Data are mean $\pm$ SE (n = 250). There were two-way interactions of adipose tissue and age on adipocyte size ($P < 0.001$) and number ($P < 0.05$). Bars with different letters are significantly different ($P < 0.05$).

abundance of lipid metabolic genes in SAT and AAT development were determined (Figure 6). Among lipid uptake genes (Figure 6A), the level in *LPL* was markedly upregulated, and increased 13-fold and 9-fold in SAT and AAT, respectively. The expression of *ap2/ FABP4* and *ACSL1* in AAT and SAT had a similar pattern of increased and then decreased expression. Next, we compared the expression levels of the genes for key lipogenesis, including *PPARα*, *PPARγ* and *FAS*, between AAT and SAT (Figure 6B). The expression of *PPARα*, *PPARγ* and *FAS* in SAT had a similar pattern of increased and then decreased expression. The expression of *PPARγ* and *FAS* in AAT was markedly downregulated ($P < 0.05$), whereas the *PPARα* mRNA level was markedly upregulated ($P < 0.05$). Then, we also examined the expression levels of lipolysis genes including *ATGL* and *IL-6* (Figure 6C). The expression levels of *ATGL* increased during development until they reached their maximum point at P70, and it declined subsequently in AAT and SAT. Meanwhile, the gene expression level of *IL-6* elevated ($P = 0.016$) from E20 to E30 and then declined in AAT ($P = 0.017$). No major expression trend was observed in SAT for the *IL-6* gene throughout the whole development ($P = 0.853$).

DISCUSSION

Adipose tissue is the body's most important energy storage organ. In chickens and some other avian species, adipose tissue is mainly found in the abdominal and beneath the skin areas, as well as the subcutaneous regions (Saarela et al., 1989). Excessive abdominal or subcutaneous fat is considered to be a by-product because the bulk of it is discarded; it both causes difficulty in meat processing and compromises consumer acceptance. Most importantly, the deposition of abdominal fat is energetically expensive and hence detracts from energy efficiency. Thus, conducting research to study regulation mechanisms of meat animal adipose tissue growth and development was imperative to develop
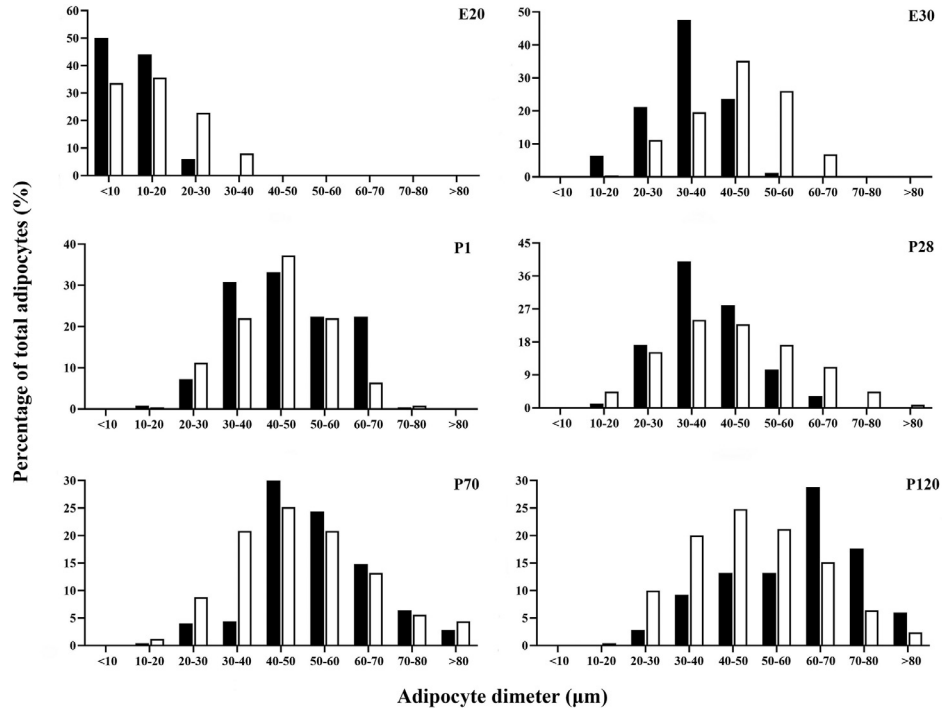
Figure 5. Number frequency distribution of adipocytes in abdominal (black bars) and subcutaneous adipose (white bars) tissue (n = 250).

strategies for decreasing abdominal or subcutaneous adipose tissue accretion. However, not all adipose is equal, and the impact of heterogeneity on the development and expansion of different adipose depots is becoming increasingly apparent (Cleal et al., 2017). In this study,

the first adipose deposit was observed near the leg between E10 and E15, and development of AAT in goose could be ascertained between E15 and E20. Similar observations were also obtained in chickens, in which SAT appears as early as d 9 of incubation and forms
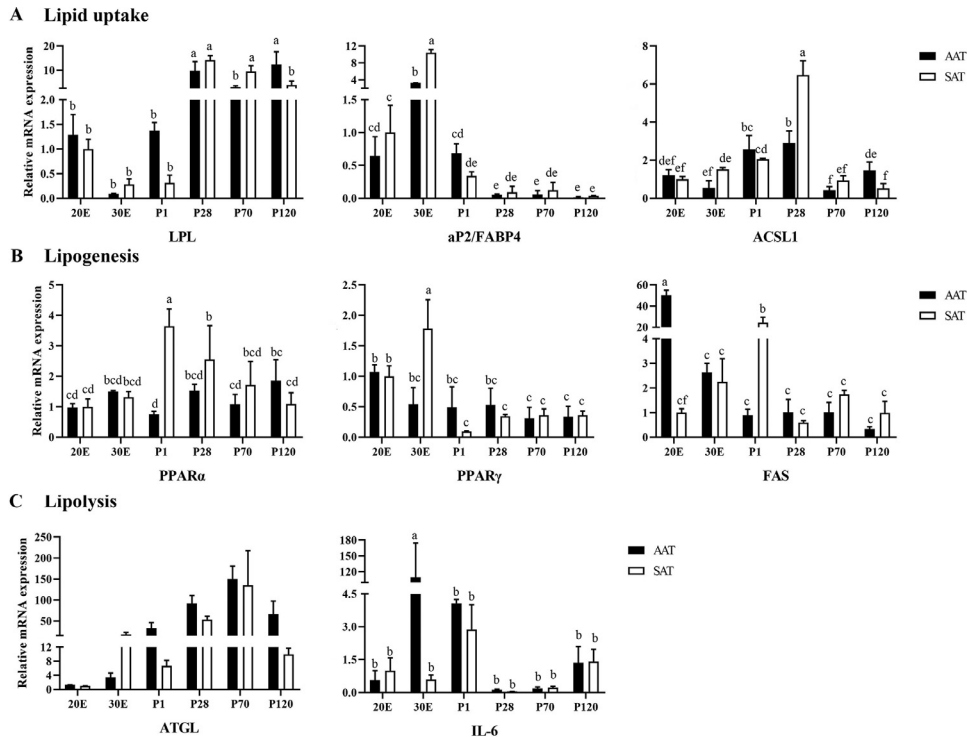
Figure 6. Expression levels of lipid metabolic genes in abdominal (AAT) and subcutaneous adipose tissue (SAT). (A) Expression levels of fatty acid transport lipoprotein lipase (LPL), fatty acid binding protein 4 (FABP4/aP2), and long-chain acyl-CoA synthetase 1 (ACSL1) genes. (B) Expression levels of peroxisome proliferator-activated receptor-α/γ (PPARα/γ) and fatty acid synthase (FAS). (C) Expression levels of adipose triglyceride lipase (ATGL) and interleukin-6 (IL-6). Data are expressed as means±SE. There were two-way interactions of tissue and age ($P < 0.01$) on mRNA abundance for all genes examined in this study, except ATGL (no two-way interactions, $P = 0.155$). Bars with different letters are significantly different ($P < 0.05$).

earlier than AAT (Chen et al., 2014; Bai et al., 2015). However, unlike the continuous accumulation with increasing speed as body weights increased in AAT with age, the increase of fat weight in SAT seems to stop after P70, indicating that SAT might be an early maturing adipose tissue, which is beneficial for the maintenance of body temperature of geese in early growth.

In periods of chronic positive energy imbalance, adipocytes store surplus energy, expanding in size of adipocytes (hypertrophy) and in number of adipocytes (hyperplasia) as a consequence (Jang et al., 2016; Cleal et al., 2017). Evidence has now accumulated that subcutaneous and abdominal adipocyte sizes are strongly related to body composition and fat distribution in pig (Nakajima et al., 2011) and chicken (Guo et al., 2011; Bai et al., 2015; Xiao et al., 2019). In this context, quantifying the number and size of adipocytes in the development and deposition is essential in characterizing the phenotype of a given adipose tissue depot. In the present study, we found that increases in the weight of the adipose depots coincided with increases in adipocyte size, whereas the proliferation of adipocytes decreased from E20 to P120 also agrees with previous reports (Bai et al., 2015). Therefore, we speculate that adipocyte hypertrophy appears to occur in a continuous manner and hypertrophic growth gradually became dominant. It is well established that the benefit of using a frequency distribution rather than the average adipocyte area alone emerges, whereas the overall average area of the adipocytes may not change, the number of adipocytes of a given size may be altered (Nakajima et al., 2011; Parlee et al., 2014). In this case, the number of total adipocytes within the distribution is subsequently calculated and used to convert the frequency to a percentage of total adipocytes counted. There was a biphasic diameter distribution of SAT and AAT, and small cells appeared throughout the ages coincide with those previous reports in pigs (Nakajima et al., 2011). This suggests that the geese adipose tissue comprises various stages of adipocytes. Although the size of adipocytes in AAT keeps increasing, the increase of fat cell size in SAT seems to stop after P70. To conclude, we found that the cellularity differences exist between SAT and AAT, and adipocyte hypertrophy is the most overwhelming contributor to the adipose deposition for geese.

Adipose tissue is the primary site in the body for storage of energy, and surplus energy mainly in the form of triacylglycerols. A study demonstrated that the lipid content of adipose tissue gradually increased at early stages and slightly decreased at later stages in broiler chickens (Foglia et al., 1994). In contrast to broiler chickens, we found that the TG content in SAT and AAT showed a"rise, decline and rise" trend. The discrepancy may result from our use of samples from multiple regions of adipose tissue rather than from a single specific location, as described by Kou et al. (2012). As the TG content reflects the fat storage capacity, our findings suggest that AAT may display greater fat storage capacity than the SAT from P28 to P120. Consistent with our results, Tchoukalova et al. (2010) also give explanation for this phenomenon that many region specific differences in abilities to store lipids.

Based on the above study, our studies and others have demonstrated that the difference in developmental dynamics between SAT and AAT in goose. This may be because the deposition of AAT and SAT are subject to different regulatory mechanisms (Schoettl et al., 2018). Numerous studies in livestock and chickens have reported the deposition of adipose tissue is determined by a balance between fat deposition and fat removal (Arner, 2018). To understand the mechanisms underlying fat deposition and fat removal in SAT and AAT, we investigated the expression of genes involved in lipid uptake, lipogenesis, and lipolysis. It is well known that *LPL* is a rate-limiting enzyme for the hydrolysis of the TG, and LPL-catalyzed reaction products, fatty acids and monoacylglycerol, are taken up, in part, by adipose tissue and stored as neutral lipids (Wang et al., 2009). *FABP4* is also associated with fat levels, and is involved in fatty acid uptake, transport, and metabolism (Lee et al., 2017). *ACSL1*, is a key enzyme in the lipid metabolism, which is involved in the regulation of uptake (Digel et al., 2009). *FAS* is transcriptionally regulated and a key enzyme in fatty acid synthesis (Jensen-Urstad et al., 2012). Both *PPARα* and *PPARγ* mainly influences fatty acid metabolism and its activation lowers lipid levels, and they modulate the lipid accumulation via increased expression of *LPL* (Bocher et al., 2002). *ATGL* is a recently discovered triglyceride lipase that hydrolyzes the first ester bond of stored TG (Zechner et al., 2009). It is reported that *IL-6* is a cytokine implicated in the regulation of energy metabolism (Theurich et al., 2017). In vitro studies in adipocytes have confirmed *IL-6* stimulates lipolysis (Carey et al., 2006). In the present study, we found that SAT had higher levels of mRNA for the lipid uptake, lipogenesis genes than AAT, whereas relative expression level of lipolysis gene was higher in AAT during embryonic stages. It was suggested that the high rate of lipolysis in AAT prevented fat accumulation in the embryonic days. These findings were consistent with Calabotta et al. (1985). After birth, the increased expression of *LPL* and *PPARα* in AAT indicated that lipogenic capacity may increase, whereas *AGTL* expression decreased. Therefore, we found that increased lipid uptake, lipogenesis and decreased lipolysis contribute to increased AAT deposition.

In conclusion, the findings of the present study provides sufficient evidence that the difference in developmental dynamics between SAT and AAT in goose. Considering that there is disparity in development, cellularity and metabolic function of the adipose tissues, we suggest that careful consideration for the precise method used to control SAT or AAT deposition in meat-producing animals to improved feed efficiency. In addition, it should be noted that our study only focused on the major adipose tissue depots in goose, whereas fat is also a critical component of tissues including liver and skeletal muscle. Our continued research efforts will focus

on fat mass changes in other tissues may compliment and provide better understanding of contributions from each component to the overall body fat mass during development.

ACKNOWLEDGMENTS

DISCLOSURES

None of the authors involved in this research have any conflicts of interest to report.

SUPPLEMENTARY MATERIALS

Supplementary material associated with this article can be found in the online version at doi:10.1016/j.psj.2021.101185.

REFERENCES

Arner, P. 2018. Fat tissue growth and development in humans. Nestle Nutr. Inst. Workshop Ser. 89:37–45.

Bai, S., G. Wang, W. Zhang, S. Zhang, B. B. Rice, M. A. Cline, and E. R. Gilbert. 2015. Broiler chicken adipose tissue dynamics during the first two weeks post-hatch. Comp. Biochem. Physiol. A Mol. Integr. Physiol. 189:115–123.

Billon, N., and C. Dani. 2012. Developmental origins of the adipocyte lineage: new insights from genetics and genomics studies. Stem Cell Rev. Rep. 8:55–66.

Bocher, V., I. Pineda-Torra, J. C. Fruchart, and B. Staels. 2002. PPARs: transcription factors controlling lipid and lipoprotein metabolism. Ann. N. Y. Acad. Sci. 967:7–18.

Calabotta, D. F., J. A. Cherry, P. B. Siegel, and D. E. Jones. 1985. Lipogenesis and lipolysis in fed and fasted chicks from high and low body weight lines. Poult. Sci. 64:700–704.

Cannon, B., and J. Nedergaard. 2004. Brown adipose tissue: function and physiological significance. Physiol. Rev. 84:277–359.

Carey, A., G. Steinberg, S. Macaulay, W. Thomas, A. Holmes, G. Ramm, and M. Febbraio. 2006. Interleukin-6 increases insulin-stimulated glucose disposal in humans and glucose uptake and fatty acid oxidation in vitro via amp-activated protein kinase. Diabetes 55:2688–2697.

Chen, P., Y. Suh, Y. M. Choi, S. Shin, and K. Lee. 2014. Developmental regulation of adipose tissue growth through hyperplasia and hypertrophy in the embryonic Leghorn and broiler. Poult. Sci. 93:1809–1817.

Cleal, L., T. Aldea, and Y. Y. Chau. 2017. Fifty shades of white: understanding heterogeneity in white adipose stem cells. Adipocyte 6:205–216.

Digel, M., R. Ehehalt, W. Stremmel, and J. Füllekrug. 2009. Acyl-CoA synthetases: fatty acid uptake and metabolic channeling. Mol. Cell. Biochem. 326:23–28.

FAO-STAT. 2020. Food and agriculture organization of the united nations. Livestock Primary. http://www.fao.org/faostat/en/#data/QL.

Foglia, T. A., A. L. Cartwright, R. J. Gyurik, and J. G. Philips. 1994. Fatty acid turnover rates in the adipose tissues of the growing chicken (Gallus domesticus). Lipids 29:497–502.

Guo, L., B. Sun, Z. Shang, Z. Shang, L. Leng, Y. Wang, N. Wang, and H. Li. 2011. Comparison of adipose tissue cellularity in chicken lines divergently selected for fatness. Poult. Sci. 90:2024–2034.

Jang, H., M. Kim, S. Lee, J. Kim, D. C. Woo, K. W. Kim, and I. Lee. 2016. Adipose tissue hyperplasia with enhanced adipocyte-derived stem cell activity in Tc1(C8orf4)-deleted mice. Sci. Rep. 6:35884.

Jensen-Urstad, A. P., and C. F. Semenkovich. 2012. Fatty acid synthase and liver triglyceride metabolism: housekeeper or messenger? Biochim. Biophys. Acta 1821:747–753.

Kou, J., W. X. Wang, H. H. Liu, Z. X. Pan, T. He, J. W. Hu, and J. W. Wang. 2012. Comparison and characteristics of the formation of different adipose tissues in ducks during early growth. Poult. Sci. 91:2588–2597.

Lee, Y. S., J. Y. Kim, K. S. Oh, and S. W. Chung. 2017. Fatty acid-binding protein 4 regulates fatty infiltration after rotator cuff tear by hypoxia-inducible factor 1 in mice. J. Cachexia Sarcopenia Muscle 8:839–850.

Liu, B. Y., Z. Y. Wang, H. M. Yang, J. M. Wang, D. Xu, R. Zhang, and Q. Wang. 2011. Influence of rearing system on growth performance, carcass traits, and meat quality of Yangzhou geese. Poult. Sci. 90:653–659.

Liu, H. X., Y. Hu, G. G. Ji, and H. F. Li. 2014. Rapid-sexing poultries via a new pair of universal primers. Chin. J. Agric. Biotechol. 22:1567–1574.

Livak, K. J., and T. D. Schmittgen. 2001. Analysis of relative gene expression data using real-time quantitative PCR and the 2(-Delta Delta C(T)). Method. Methods. 25:402.

Lu, L., Y. Chen, Z. Wang, X. Li, W. Chen, Z. Tao, and J. Wang. 2015. The goose genome sequence leads to insights into the evolution of waterfowl and susceptibility to fatty liver. Genome Biol. 16:89.

Majka, S. M., Y. Barak, and D. J. Klemm. 2011. Concise review: adipocyte origins: weighing the possibilities. Stem Cells 29:1034–1040.

Nakajima, I., M. Oe, K. Ojima, S. Muroya, M. Shibata, and K. Chikuni. 2011. Cellularity of developing subcutaneous adipose tissue in Landrace and Meishan pigs: adipocyte size differences between two breeds. Anim. Sci. J. 82:144–149.

Orkusz, A., G. Haraf, A. Okruszek, and M. Werenska-Sudnik. 2017. Lipid oxidation and color changes of goose meat stored under vacuum and modified atmosphere conditions. Poult. Sci. 96:731–737.

Parlee, S. D., S. I. Lentz, H. Mori, and O. A. MacDougald. 2014. Quantifying size and number of adipocytes in adipose tissue. Methods Enzymol. 537:93–122.

Saarela, S., R. Hissa, A. Pyörnilä, R. Harjula, M. Ojanen, and M. Orell. 1989. Do birds possess brown adipose tissue? Comp. Biochem. Physiol. 92:219–228.

Schoettl, T., I. P. Fischer, and S. Ussar. 2018. Heterogeneity of adipose tissue in development and metabolic function. J. Exp. Biol. 7:221.

Tchoukalova, Y. D., S. B. Votruba, T. Tchkonia, N. Giorgadze, J. L. Kirkland, and M. D. Jensen. 2010. Regional differences in cellular mechanisms of adipose tissue gain with overfeeding. Proc. Natl. Acad. Sci. U. S. A. 107:18226–18231.

Theurich, S., E. Tsaousidou, R. Hanssen, A. M. Lempradl, J. Mauer, K. Timper, and V. Sexl. 2017. IL-6/Stat3-Dependent induction of a distinct, obesity-associated nk cell subpopulation deteriorates energy and glucose homeostasis. Cell Metab. 26:171–184.

Wang, Y. H., N. I. Bower, A. Reverter, S. H. Tan, N. De Jager, R. Wang, and S. A. Lehnert. 2009. Gene expression patterns during intramuscular fat development in cattle. J. Anim. Sci. 87:119–130.

Wang, Z. Y., S. R. Shi, Q. Y. Zhou, H. M. Yang, J. M. Zou, K. N. Zhang, and H. M. Han. 2010. Response of growing goslings to dietary methionine from 28 to 70 days of age. Br. Poult. Sci. 51:118–121.

Webster, R. G., W. J. Bean, O. T. Gorman, T. M. Chambers, and Y. Kawaoka. 1992. Evolution and ecology of influenza A viruses. Microbiol. Rev. 56:152–179.

Wronska, A., and Z. Kmiec. 2012. Structural and biochemical characteristics of various white adipose tissue depots. Acta Physiol. (Oxf) 205:194–208.

Xiao, Y., G. Wang, M. E. Gerrard, S. Wieland, M. Davis, M. A. Cline, and E. R. Gilbert. 2019. Changes in adipose tissue physiology during the first two weeks posthatch in chicks from lines selected for low or high body weight. Am. J. Physiol. Regul. Integr. Comp. Physiol. 316:802–818.

Yu, J., H. M. Yang, Y. Y. Lai, X. L. Wan, and Z. Y. Wang. 2020. The body fat distribution and fatty acid composition of muscles and adipose tissues in geese. Poult. Sci. 99:4634–4641.

Zechner, R., P. C. Kienesberger, G. Haemmerle, R. Zimmermann, and A. Lass. 2009. Adipose triglyceride lipase and the lipolytic catabolism of cellular fat stores. J. Lipid Res. 50:3–21.

Zhang, J., Y. Suh, Y. M. Choi, P. R. Chen, M. E. Davis, and K. Lee. 2015. Differential expression of cell cycle regulators during hyperplastic and hypertrophic growth of broiler subcutaneous adipose tissue. Lipids 50:965–976.